

# Second-order nonlinear optical (NLO) polymers containing perfluoroaromatic rings as isolation groups with Ar/Ar<sup>F</sup> self-assembly effect: Enhanced NLO coefficient and stability



Wenbo Wu<sup>a</sup>, Qi Huang<sup>a</sup>, Cheng Zhong<sup>a</sup>, Cheng Ye<sup>b</sup>, Jingui Qin<sup>a</sup>, Zhen Li<sup>a,\*</sup>

<sup>a</sup> Department of Chemistry, Hubei Key Lab on Organic and Polymeric Opto-Electronic Materials, Wuhan University, Wuhan 430072, China

<sup>b</sup> Organic Solids Laboratories, Institute of Chemistry, The Chinese Academy of Sciences, Beijing 100080, China

## ARTICLE INFO

### Article history:

Received 26 March 2013  
Received in revised form  
26 May 2013  
Accepted 27 July 2013  
Available online 6 August 2013

### Keywords:

Nonlinear optics (NLO)  
Isolation groups  
Ar/Ar<sup>F</sup> self-assembly effect

## ABSTRACT

Four new polyaryleneethylenes **P1–P4**, which contained different aromatic or perfluoroaromatic isolation groups, were successfully prepared, via the palladium-catalyzed Sonogashira coupling reaction. Among them, **P2**, due to the presence of the self-assembly effect between the perfluoroaromatic and chromophore moieties, demonstrated much larger NLO effect ( $d_{33}$  value of 162.3 pm/V) and better stability with onset temperature for decay (111 °C). The research on the polymer conformation suggested that perfluorophenyl groups in different positions would result in different effects on the NLO coefficient, providing some useful information for the design of NLO polymers with better performance.

© 2013 Elsevier Ltd. All rights reserved.

## 1. Introduction

Organic second-order nonlinear optical (NLO) materials have attracted much attention among scientists for their potential applications in photonics, due to their large NLO coefficients, ultrafast response time and ease of integration, in comparison with conventional inorganic NLO crystals (such as LiNbO<sub>3</sub> and so on) [1]. One of the major problems encountered in optimizing organic NLO materials is how to efficiently translate the high  $\mu\beta$  values of the organic chromophores into large macroscopic NLO activities of polymers [2]. To solve this problem, it is badly needed to overcome or minimize the strong intermolecular dipole–dipole interactions among the NLO chromophore moieties to achieve their orderly alignment upon poling. Just this interaction accounts for the fact that the NLO properties of the polymers are only enhanced several times even if the  $\mu\beta$  values of chromophores have been improved by up to 250-fold. Fortunately, it has been proved to be an efficient approach for minimizing this interaction and enhancing the poling efficiency to introduce isolation groups into chromophores to further control the shape of the chromophores, with spherical shape, proposed by Dalton and Jen et al., being the most ideal conformation [3]. Based on the excellent work of pioneer scientists

in the NLO field and according to the site isolation principle [4], from 2006, our group have designed many different types of NLO dendronized polymers containing different isolation groups with different size in the chromophore moieties (Charts S1–S6 in the Supporting information). Based on the obtained experimental results, we proposed the concept of “suitable isolation group”, for the design of NLO polymers with good performance [5].

However, nearly all the isolation groups in the previous cases were only designed to adjust the shape of the chromophore and decrease the strong interactions between the chromophore moieties, and few reports were concerned on the interactions between chromophore and isolation group or different isolation groups. Different from normal aromatic rings, perfluoroaromatic rings were electropositive, and this activity could lead to the reversible self-assembly of the two types of aromatic rings, perfluoroaromatic and normal aromatic ones [6]. For example, it has been determined that the structure of the benzene/hexafluorobenzene mixture consists of alternating stacks of these two molecules, while pure benzene or pure hexafluorobenzene adopts an edge-to-face structure in the solid-state (Chart S7). Recently, this Ar–Ar<sup>F</sup> self-assembly effect has been successfully applied to NLO materials, by Jen and co-workers in 2007: they developed a new class of molecular glasses (Chart S8), by utilizing aromatic/perfluoroaromatic dendron-substituted NLO chromophores through the presence of complementary Ar/Ar<sup>F</sup> interactions, which exhibited the improved poling efficiency and much enhanced macroscopic NLO effects [7]. Two

\* Corresponding author. Fax: +86 27 68756757.

E-mail addresses: [lizhen@whu.edu.cn](mailto:lizhen@whu.edu.cn), [lichemlab@163.com](mailto:lichemlab@163.com) (Z. Li).

years later, they observed the same phenomenon again in another series of dendritic NLO chromophores containing perfluoroaromatic moieties (Chart S9) [8]. This method was also applied into NLO polymers and dendrimers by us, and the highest NLO effect ( $d_{33}$  value up to 166.7 pm/V) so far for linear polymers was achieved by using simple azo chromophore (Chart S10) [9]. However, till now, the successful example was still very scarce, possibly due to the unclear self-assembly behavior in the NLO polymers.

In this paper, we attempted to investigate the interactions between perfluoroaromatic moieties and other normal aromatic moieties in NLO polymers, and their influence on the macroscopic NLO effect in detail. Therefore, four polyaryleneethynylenes (**P1–P4**) were synthesized (Scheme 1), in which the isolation groups were elaborately designed as either aromatic or perfluoroaromatic ones. The tested NLO properties demonstrated that the position of the perfluoroaromatic groups affected the NLO effects of the polymers in a large degree. The theoretical calculation research also supported this point. Furthermore, thanks to the Ar/Ar<sup>F</sup> self-assembly effect, the stability of NLO effects was improved. Herein, we would like to present the syntheses, characterization and properties of these polymers in detail.

## 2. Experimental section

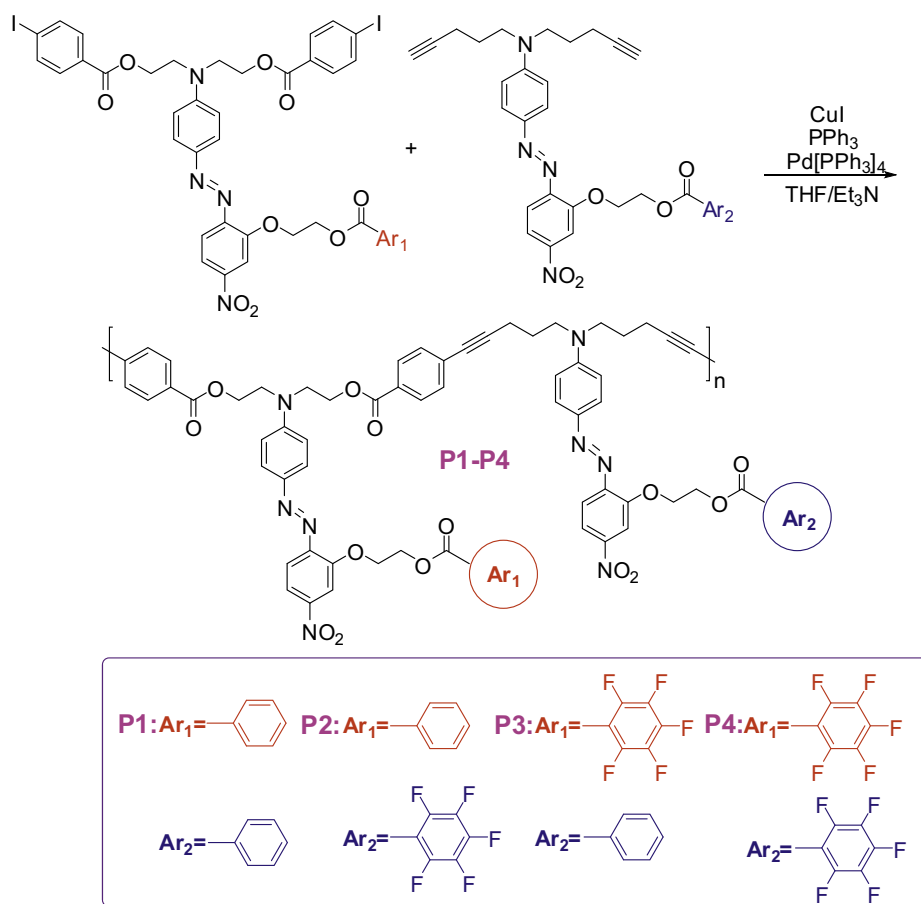
### 2.1. Materials

Tetrahydrofuran (THF) was dried over and distilled from K–Na alloy under an atmosphere of dry nitrogen. Triethylamine (Et<sub>3</sub>N) was distilled under normal pressure and kept over potassium

hydroxide. Dichloromethane (CH<sub>2</sub>Cl<sub>2</sub>, DCM) was dried over from CaH<sub>2</sub> and distilled under normal pressure before use. Diazonium fluoroborate (**3**) [10] and *N,N*-di(4-pentynyl)benzenamine (**5**) [5f] were synthesized according to the literature method. 4-Iodobenzoic acid and pentafluorobenzoic acid were purchased from Alfa-Aesar. *N*-Phenyldiethanol (**1**) was bought from Fluka. All other reagents were used as received.

### 2.2. Instrumentation

<sup>1</sup>H and <sup>13</sup>C NMR spectra were measured on a Varian Mercury300 or Bruker ARX 400 spectrometer using tetramethylsilane (TMS;  $\delta = 0$  ppm) as internal standard. <sup>19</sup>F NMR spectra were measured on a Varian Mercury600 spectrometer. The Fourier transform infrared (FT-IR) spectra were recorded on a PerkinElmer-2 spectrometer in the region of 3000–400 cm<sup>-1</sup>. UV–visible spectra were obtained using a Shimadzu UV-2550 spectrometer. Elemental analyses (EA) were performed by a CARLOERBA-1106 microelemental analyzer. Gel permeation chromatography (GPC) was used to determine the molecular weights of polymers. GPC analysis was performed on a Waters HPLC system equipped with a 2690D separation module and a 2410 refractive index detector. Polystyrene standards were used as calibration standards for GPC. THF was used as an eluent, and the flow rate was 1.0 mL/min. Thermal analysis was performed on NETZSCH STA449C thermal analyzer at a heating rate of 10 °C/min in nitrogen at a flow rate of 50 cm<sup>3</sup>/min for thermogravimetric analysis (TGA) and the thermal transitions of the polymers. The thickness of the films was measured with an Ambios Technology XP-2 profilometer.



Scheme 1. The synthesis of NLO polymers.

### 2.3. Synthesis of compound 2

*N*-Phenyldiethanolamin (**1**) (1.08 g, 6.0 mmol), 4-iodobenzoic acid (4.46 g, 18.0 mmol), 1-(3-dimethylaminopropyl)-3-ethyl carbodiimide hydrochloride (EDC) (4.60 g, 24.0 mmol), and 4-(*N,N*-dimethyl)aminopyridine (DMAP) (288 mg, 2.40 mmol) were dissolved in dry CH<sub>2</sub>Cl<sub>2</sub> (120 mL) and stirred at room temperature for 3 days, and then treated with saturated solution of citric acid and extracted with CH<sub>2</sub>Cl<sub>2</sub>, washed with brine and saturated solution of citric acid. After the removal of all the solvent, the crude product was recrystallized from a lot of acetone to afford white solid (3.80 g, 98.8%). <sup>1</sup>H NMR (300 MHz, DMSO-*d*<sub>6</sub>, 298 K),  $\delta$  (TMS, ppm): 3.79 (t, *J* = 5.1 Hz, 4H, -NCH<sub>2</sub>-), 4.41 (t, *J* = 5.1 Hz, 4H, -OCH<sub>2</sub>-), 6.63 (t, *J* = 7.2 Hz, 1H, ArH), 6.88 (d, *J* = 8.4 Hz, 2H, ArH), 7.17 (t, *J* = 7.8 Hz, 2H, ArH), 7.63 (d, *J* = 8.1 Hz, 4H, ArH), 7.87 (d, *J* = 8.1 Hz, 4H, ArH). <sup>13</sup>C NMR (75 MHz, DMSO-*d*<sub>6</sub>, 298 K),  $\delta$  (ppm): 50.4, 64.1, 103.6, 113.7, 117.9, 130.6, 130.8, 132.5, 139.3, 149.0, 167.1.

### 2.4. Synthesis of compound 4

Compound **2** (962 mg, 1.50 mmol) and diazonium salt (**3**) (668 mg, 2.25 mmol) were dissolved in DMF/THF (15 mL/15 mL) at 0 °C. The reaction mixture was stirred for 36 h at 0 °C, and then treated with H<sub>2</sub>O and extracted with a lot of CHCl<sub>3</sub>, washed with brine. The organic layer was dried over anhydrous sodium sulfate. After the removal of the organic solvent, the crude product was purified by column chromatography on silica gel using ethyl acetate/petroleum ether (2/3, v/v) as eluent and then recrystallized from ethyl acetate to afford red solid (920 mg, 72.2%). <sup>1</sup>H NMR (400 MHz, CDCl<sub>3</sub>, 298 K),  $\delta$  (TMS, ppm): 3.83 (s, br, 2H, -OCH<sub>2</sub>-), 3.98 (s, br, 4H, -NCH<sub>2</sub>-), 4.32 (s, br, 4H, -OCH<sub>2</sub>-), 5.0 (s, 1H, -OH), 7.09 (d, *J* = 9.0 Hz, 2H, ArH), 7.64 (m, 5H, ArH), 7.85 (m, 7H, ArH), 8.01 (s, 1H, ArH). <sup>13</sup>C NMR (75 MHz, CDCl<sub>3</sub>, 298 K),  $\delta$  (ppm): 49.6, 60.2, 63.1, 72.3, 102.8, 110.5, 112.9, 117.9, 126.4, 129.5, 131.5, 138.4, 144.6, 147.0, 148.5, 152.1, 155.7, 166.1.

### 2.5. Synthesis of compound 6

*N,N*-Di(4-pentynyl)benzenamine (**5**) (901.3 mg, 4.0 mmol) and diazonium salt (**3**) (1.19 g, 4.0 mmol) were dissolved in DMF at 0 °C. The reaction mixture was stirred for 12 h at 0 °C, and then treated with H<sub>2</sub>O and extracted with CH<sub>2</sub>Cl<sub>2</sub>, washed with brine. The organic layer was dried over anhydrous sodium sulfate. After the removal of the organic solvent, the crude product was purified by column chromatography on silica gel using ethyl acetate/petroleum ether (2/1, v/v) as eluent to afford deep red solid (1.1 g, 63.3%). <sup>1</sup>H NMR (400 MHz, CDCl<sub>3</sub>, 298 K),  $\delta$  (TMS, ppm): 1.88 (m, 4H, -CH<sub>2</sub>-), 2.05 (s, 2H, -C≡C-H), 2.30 (m, 4H, -CH<sub>2</sub>-), 3.59 (t, *J* = 6.0 Hz, 4H, -NCH<sub>2</sub>-), 4.00 (t, *J* = 4.0 Hz, 2H, -OCH<sub>2</sub>-), 4.37 (t, *J* = 4.0 Hz, 2H, -OCH<sub>2</sub>-), 6.80 (d, *J* = 8.0 Hz, 2H, ArH), 7.72 (d, *J* = 8.0 Hz, 1H, ArH), 7.86 (d, *J* = 8.0 Hz, 2H, ArH) 7.95 (m, 2H, ArH).

### 2.6. General procedure for the synthesis of chromophores C1–C4

Compound **4** or **6** (1.00 equiv.), carboxyl-containing compound (1.50 equiv.), 1-(3-dimethylaminopropyl)-3-ethylcarbodiimide hydrochloride (EDC) (2.00 equiv.), and 4-(*N,N*-dimethyl)aminopyridine (DMAP) (0.20 equiv.) were dissolved in dry CH<sub>2</sub>Cl<sub>2</sub> (0.1 mmol/mL of compound **4** or **6**) and stirred at room temperature for 3 h, and then treated with saturated solution of citric acid and extracted with CH<sub>2</sub>Cl<sub>2</sub>, washed with brine and saturated solution of citric acid. After the removal of the solvent, the crude product was purified by column chromatography on silica gel.

#### 2.6.1. Chromophore C1

Compound **4** (425.2 mg, 0.50 mmol), benzoic acid (91.6 mg, 0.75 mmol). The crude product was purified by column chromatography on silica gel using ethyl acetate/chloroform (1/15, v/v) as eluent to afford deep red solid (459.6 mg, 96.2%). IR (KBr),  $\nu$  (cm<sup>-1</sup>): 1719 (C=O), 1517, 1338 (-NO<sub>2</sub>). <sup>1</sup>H NMR (400 MHz, CDCl<sub>3</sub>, 298 K),  $\delta$  (TMS, ppm): 3.91 (t, *J* = 8.0 Hz, 4H, -NCH<sub>2</sub>-), 4.55 (t, *J* = 8.0 Hz, 4H, -COOCH<sub>2</sub>-), 4.63 (t, *J* = 4.0 Hz, 2H, -OCH<sub>2</sub>-), 4.81 (t, *J* = 4.0 Hz, 2H, -COOCH<sub>2</sub>-), 6.89 (d, *J* = 8.0 Hz, 2H, ArH), 7.39 (d, *J* = 8.0 Hz, 2H, ArH), 7.53 (d, *J* = 8.0 Hz, 1H, ArH), 7.69 (m, 5H, ArH), 7.79 (d, *J* = 8.0 Hz, 4H, ArH), 7.90 (m, 3H, ArH), 8.04 (m, 3H, ArH). <sup>13</sup>C NMR (75 MHz, CDCl<sub>3</sub>, 298 K),  $\delta$  (ppm): 49.5, 61.6, 62.8, 68.4, 101.1, 110.3, 111.6, 117.0, 117.4, 126.0, 128.1, 128.6, 129.5, 130.7, 132.9, 137.6, 144.8, 147.0, 148.0, 150.5, 154.8, 165.7. C<sub>39</sub>H<sub>32</sub>N<sub>4</sub>O<sub>9</sub>I<sub>2</sub> (EA) (% found/calcd): C, 48.82/49.07; H, 3.82/3.38; N, 5.80/5.87. UV-vis (THF, 1 × 10<sup>-5</sup> mmol/mL):  $\lambda_{\max}$  (nm): 465.

#### 2.6.2. Chromophore C2

Compound **4** (425.2 mg, 0.50 mmol), pentafluorobenzoic acid (159.1 mg, 0.75 mmol). The crude product was purified by column chromatography on silica gel using ethyl acetate/chloroform (1/15, v/v) as eluent to afford red solid (439.0 mg, 84.1%). IR (KBr),  $\nu$  (cm<sup>-1</sup>): 1721 (C=O), 1518, 1337 (-NO<sub>2</sub>). <sup>1</sup>H NMR (400 MHz, CDCl<sub>3</sub>, 298 K),  $\delta$  (TMS, ppm): 3.91 (t, *J* = 8.0 Hz, 4H, -NCH<sub>2</sub>-), 4.57 (m, 6H, -COOCH<sub>2</sub>- and -OCH<sub>2</sub>-), 4.88 (t, *J* = 4.0 Hz, 2H, -COOCH<sub>2</sub>-), 6.92 (d, *J* = 8.0 Hz, 2H, ArH), 7.69 (m, 5H, ArH), 7.79 (d, *J* = 8.0 Hz, 4H, ArH), 7.88 (d, *J* = 8.0 Hz, 2H, ArH), 7.95 (m, 2H, ArH). <sup>13</sup>C NMR (75 MHz, CDCl<sub>3</sub>, 298 K),  $\delta$  (ppm): 15.6, 25.4, 49.6, 62.8, 68.3, 69.2, 82.7, 110.3, 111.1, 117.1, 117.2, 126.1, 128.0, 129.4, 132.8, 144.0, 147.6, 150.8, 154.5. <sup>19</sup>F NMR (564 MHz, CDCl<sub>3</sub>, 298 K),  $\delta$  (ppm): -137.77, -148.27, -160.61. C<sub>39</sub>H<sub>27</sub>N<sub>4</sub>O<sub>9</sub>F<sub>5</sub>I<sub>2</sub> (EA) (% found/calcd): C, 44.42/44.85; H, 2.98/2.61; N, 5.56/5.36. UV-vis (THF, 1 × 10<sup>-5</sup> mmol/mL):  $\lambda_{\max}$  (nm): 463.

#### 2.6.3. Chromophore C3

Compound **6** (499.7 mg, 1.15 mmol), benzoic acid (211.3 mg, 1.73 mmol). The crude product was purified by column chromatography on silica gel using ethyl acetate/chloroform (1/20, v/v) as eluent to afford deep red solid (614.3 mg, 99.2%). IR (KBr),  $\nu$  (cm<sup>-1</sup>): 3267 (C≡C-H), 1711 (C=O), 1519, 1335 (-NO<sub>2</sub>). <sup>1</sup>H NMR (400 MHz, CDCl<sub>3</sub>, 298 K),  $\delta$  (TMS, ppm): 1.87 (m, 4H, -CH<sub>2</sub>-), 2.06 (s, 2H, -C≡C-H), 2.30 (m, 4H, -CH<sub>2</sub>-), 3.58 (t, *J* = 8.0 Hz, 4H, -NCH<sub>2</sub>-), 4.62 (t, *J* = 4.0 Hz, 2H, -OCH<sub>2</sub>-), 4.80 (t, *J* = 4.0 Hz, 2H, -COOCH<sub>2</sub>-), 6.74 (d, *J* = 8.0 Hz, 2H, ArH), 7.40 (t, *J* = 8.0 Hz, 2H, ArH), 7.55 (t, *J* = 8.0 Hz, 1H, ArH), 7.69 (d, *J* = 8.0 Hz, 1H, ArH), 7.86 (d, *J* = 8.0 Hz, 1H, ArH), 7.92 (m, 1H, ArH), 8.05 (m, 3H, ArH), 8.17 (d, *J* = 8.0 Hz, 1H, ArH). <sup>13</sup>C NMR (75 MHz, CDCl<sub>3</sub>, 298 K),  $\delta$  (ppm): 15.8, 25.6, 49.8, 63.0, 68.4, 69.5, 83.0, 110.4, 111.2, 117.3, 126.3, 128.3, 129.6, 133.0, 144.1, 147.3, 147.8, 151.0, 154.7, 166.3. C<sub>31</sub>H<sub>30</sub>N<sub>4</sub>O<sub>5</sub> (EA) (% found/calcd): C, 68.77/69.13; H, 6.06/5.61; N, 10.06/10.40. UV-vis (THF, 1 × 10<sup>-5</sup> mmol/mL):  $\lambda_{\max}$  (nm): 489.

#### 2.6.4. Chromophore C4

Compound **6** (499.7 mg, 1.15 mmol), pentafluorobenzoic acid (365.8 mg, 1.73 mmol). The crude product was purified by column chromatography on silica gel using ethyl acetate/chloroform (1/20, v/v) as eluent to afford deep red solid (686.2 mg, 94.9%). IR (KBr),  $\nu$  (cm<sup>-1</sup>): 3299 (C≡C-H), 1743 (C=O), 1516, 1336 (-NO<sub>2</sub>). <sup>1</sup>H NMR (400 MHz, CDCl<sub>3</sub>, 298 K),  $\delta$  (TMS, ppm): 1.87 (m, 4H, -CH<sub>2</sub>-), 2.05 (s, 2H, -C≡C-H), 2.30 (m, 4H, -CH<sub>2</sub>-), 3.58 (t, *J* = 8.0 Hz, 4H, -NCH<sub>2</sub>-), 4.56 (t, *J* = 4.0 Hz, 2H, -OCH<sub>2</sub>-), 4.88 (t, *J* = 4.0 Hz, 2H, -COOCH<sub>2</sub>-), 6.76 (d, *J* = 8.0 Hz, 2H, ArH), 7.69 (d, *J* = 8.0 Hz, 1H, ArH), 7.83 (d, *J* = 8.0 Hz, 2H, ArH), 7.94 (m, 2H, ArH). <sup>13</sup>C NMR (75 MHz, CDCl<sub>3</sub>, 298 K),  $\delta$  (ppm): 15.9, 25.7, 49.9, 64.2, 67.9, 69.4, 83.0, 110.2, 111.2, 117.5, 126.3, 144.1, 147.5, 147.8, 151.1, 154.4, 158.9. <sup>19</sup>F NMR

(564 MHz,  $\text{CDCl}_3$ , 298 K),  $\delta$  (ppm):  $-137.83$ ,  $-148.42$  (d,  $J = 1.7$  Hz),  $-160.67$ .  $\text{C}_{31}\text{H}_{25}\text{N}_4\text{O}_5\text{F}_5$  (EA) (% found/calcd): C, 59.24/59.66; H, 3.95/4.01; N, 8.91/8.91. UV-vis (THF,  $1 \times 10^{-5}$  mmol/mL):  $\lambda_{\text{max}}$  (nm): 489.

## 2.7. General procedure for the synthesis of P1–P4

A mixture of chromophore **C1** or **C2** (1.00 equiv.), chromophore **C3** or **C4** (1.00 equiv.), copper iodide (CuI) (5 mol-%), tetrakis(triphenylphosphine)palladium ( $\text{Pd}(\text{PPh}_3)_4$ ) (3 mol-%) and triphenylphosphine ( $\text{PPh}_3$ ) (5 mol-%) was carefully degassed and charged with argon. THF (9 mL)/ $\text{Et}_3\text{N}$  (1 mL) was then added. The reaction was stirred for 3 days at room temperature. The mixture was passed through a cotton filter and dropped into a lot of methanol. The precipitate was collected, further purified by several precipitations of its THF solution into acetone, and dried in a vacuum at  $40^\circ\text{C}$  to a constant weight.

### 2.7.1. P1

Chromophore **C1** (114.5 mg, 0.12 mmol), chromophore **C3** (64.6 mg, 0.12 mmol). **P1** was obtained as deep red powder (107.2 mg, 72.3%).  $M_w = 17\,200$ ,  $M_w/M_n = 1.99$  (GPC, polystyrene calibration). IR (KBr),  $\nu$  ( $\text{cm}^{-1}$ ): 1719 (C=O), 1517, 1338 ( $-\text{NO}_2$ ).  $^1\text{H}$  NMR (300 MHz,  $\text{CDCl}_3$ , 298 K),  $\delta$  (TMS, ppm): 1.8–2.1 ( $-\text{CH}_2-$ ), 2.4–2.6 ( $-\text{CH}_2-$ ), 3.5–4.0 ( $-\text{NCH}_2-$ ), 4.4–5.0 ( $-\text{OCH}_2-$ ), 6.7–7.0 (ArH), 7.2–7.6 (ArH), 7.6–8.1 (ArH).  $^{13}\text{C}$  NMR (75 MHz,  $\text{CDCl}_3$ , 298 K),  $\delta$  (ppm): 17.5, 26.4, 50.1, 50.7, 62.2, 63.5, 69.0, 81.5, 92.9, 101.7, 111.0, 112.3, 118.0, 126.8, 128.8, 130.2, 132.0, 133.6, 138.3, 145.5, 147.6, 155.5, 166.3, 166.8. UV-vis (THF, 0.02 mg/mL):  $\lambda_{\text{max}}$  (nm): 475.

### 2.7.2. P2

Chromophore **C1** (104.9 mg, 0.11 mmol), chromophore **C4** (69.1 mg, 0.11 mmol). **P2** was obtained as deep red powder (128.4 mg, 87.7%).  $M_w = 8200$ ,  $M_w/M_n = 1.54$  (GPC, polystyrene calibration). IR (KBr),  $\nu$  ( $\text{cm}^{-1}$ ): 1718 (C=O), 1517, 1338 ( $-\text{NO}_2$ ).  $^1\text{H}$  NMR (300 MHz,  $\text{CDCl}_3$ , 298 K),  $\delta$  (TMS, ppm): 1.7–2.0 ( $-\text{CH}_2-$ ), 2.4–2.6 ( $-\text{CH}_2-$ ), 3.3–3.9 ( $-\text{NCH}_2-$ ), 4.3–4.6 ( $-\text{OCH}_2-$ ), 4.6–4.8

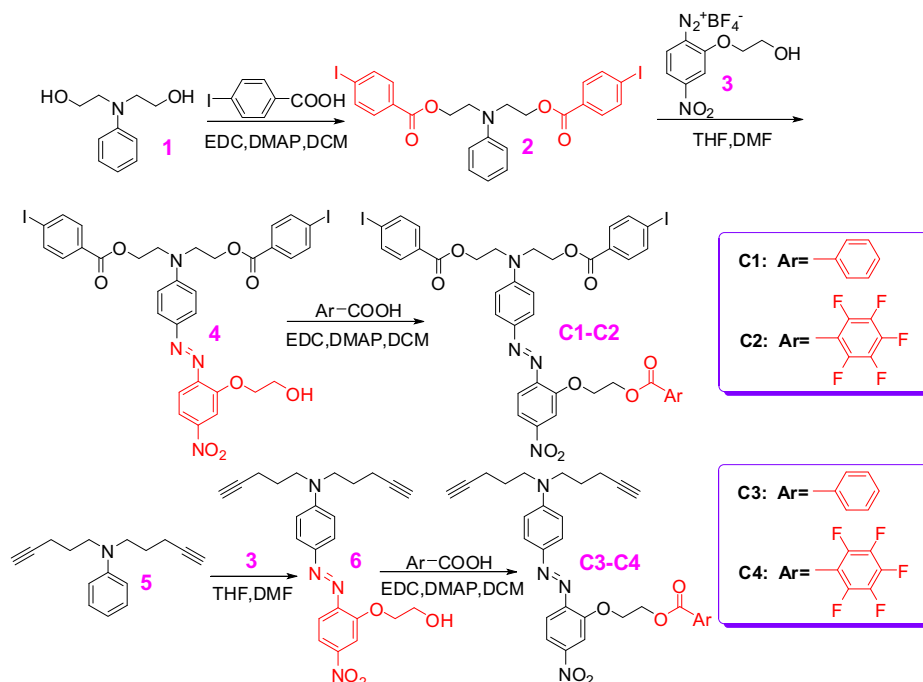
( $-\text{OCH}_2-$ ), 6.6–6.9 (ArH), 7.2–7.5 (ArH), 7.5–7.6 (ArH), 7.7–8.0 (ArH).  $^{13}\text{C}$  NMR (75 MHz,  $\text{CDCl}_3$ , 298 K),  $\delta$  (ppm): 16.1, 25.1, 48.6, 49.3, 60.7, 62.1, 63.3, 67.0, 67.8, 80.0, 91.4, 106.7, 109.6, 110.8, 116.5, 125.2, 127.3, 127.5, 128.5, 128.7, 130.0, 130.5, 131.1, 132.0, 136.8, 143.6, 145.3, 147.2, 149.9, 153.7, 157.8, 164.8.  $^{19}\text{F}$  NMR (564 MHz,  $\text{CDCl}_3$ , 298 K),  $\delta$  (ppm):  $-137.79$ ,  $-148.28$ ,  $-160.63$ . UV-vis (THF, 0.02 mg/mL):  $\lambda_{\text{max}}$  (nm): 476.

### 2.7.3. P3

Chromophore **C2** (73.1 mg, 0.07 mmol), chromophore **C3** (37.7 mg, 0.07 mmol). **P3** was obtained as deep red powder (86.3 mg, 92.4%).  $M_w = 7200$ ,  $M_w/M_n = 1.43$  (GPC, polystyrene calibration). IR (KBr),  $\nu$  ( $\text{cm}^{-1}$ ): 1720 (C=O), 1518, 1338 ( $-\text{NO}_2$ ).  $^1\text{H}$  NMR (300 MHz,  $\text{CDCl}_3$ , 298 K),  $\delta$  (TMS, ppm): 1.8–2.0 ( $-\text{CH}_2-$ ), 2.4–2.6 ( $-\text{CH}_2-$ ), 3.4–3.8 ( $-\text{NCH}_2-$ ), 3.8–4.0 ( $-\text{NCH}_2-$ ), 4.4–4.6 ( $-\text{OCH}_2-$ ), 4.6–4.9 ( $-\text{OCH}_2-$ ), 6.6–6.9 (ArH), 7.2–7.5 (ArH), 7.5–8.0 (ArH).  $^{13}\text{C}$  NMR (75 MHz,  $\text{CDCl}_3$ , 298 K),  $\delta$  (ppm): 16.8, 21.9, 25.7, 27.5, 29.4, 49.5, 61.5, 62.9, 64.0, 67.7, 68.4, 80.8, 92.0, 110.0, 111.5, 117.4, 126.0, 128.1, 128.3, 129.3, 129.5, 130.7, 131.3, 131.8, 132.9, 137.6, 144.7, 146.9, 148.0, 150.2, 154.4, 158.6, 166.0.  $^{19}\text{F}$  NMR (564 MHz,  $\text{CDCl}_3$ , 298 K),  $\delta$  (ppm):  $-137.81$ ,  $-148.46$ ,  $-160.70$ . UV-vis (THF, 0.02 mg/mL):  $\lambda_{\text{max}}$  (nm): 477.

### 2.7.4. P4

Chromophore **C2** (114.8 mg, 0.11 mmol), chromophore **C4** (69.1 mg, 0.11 mmol). **P4** was obtained as deep red powder (126 mg, 80.7%).  $M_w = 6\,600$ ,  $M_w/M_n = 1.57$  (GPC, polystyrene calibration). IR (KBr),  $\nu$  ( $\text{cm}^{-1}$ ): 1724 (C=O), 1518, 1337 ( $-\text{NO}_2$ ).  $^1\text{H}$  NMR (300 MHz,  $\text{CDCl}_3$ , 298 K),  $\delta$  (ppm): 1.8–2.1 ( $-\text{CH}_2-$ ), 2.3–2.4 ( $-\text{CH}_2-$ ), 2.4–2.6 ( $-\text{CH}_2-$ ), 3.4–3.8 ( $-\text{NCH}_2-$ ), 3.8–4.0 ( $-\text{NCH}_2-$ ), 4.4–4.7 ( $-\text{OCH}_2-$ ), 4.8–5.0 ( $-\text{OCH}_2-$ ), 6.7–6.9 (ArH), 6.9–7.0 (ArH), 7.3–7.5 (ArH), 7.6–8.0 (ArH).  $^{13}\text{C}$  NMR (75 MHz,  $\text{CDCl}_3$ , 298 K),  $\delta$  (TMS, ppm): 17.2, 26.2, 50.0, 61.9, 63.2, 64.4, 68.3, 81.2, 92.5, 111.6, 112.0, 117.7, 126.3, 128.4, 128.7, 129.6, 129.8, 131.0, 131.6, 133.1, 136.8, 137.9, 144.7, 146.5, 151.0, 154.6, 158.9, 165.9.  $^{19}\text{F}$  NMR (564 MHz,  $\text{CDCl}_3$ , 298 K),  $\delta$  (ppm):  $-137.81$ ,  $-148.27$ ,  $-160.65$ . UV-vis (THF, 0.02 mg/mL):  $\lambda_{\text{max}}$  (nm): 475.



Scheme 2. The synthesis of monomers C1–C4.

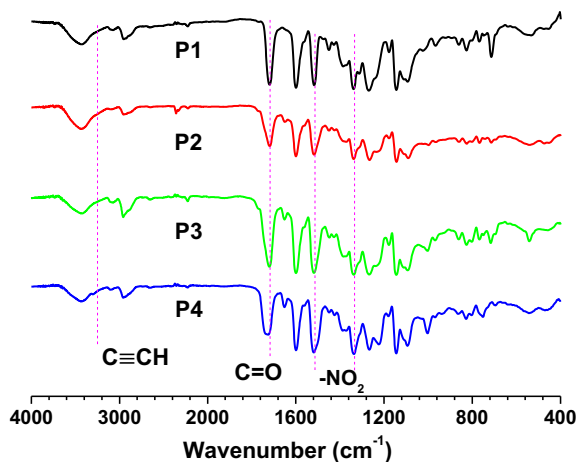


Fig. 1. The FT-IR spectra of polymer P1–P4.

### 2.8. Preparation of polymer thin films

The polymers were dissolved in THF (concentration ~3 wt %), and the solutions were filtered through syringe filters. Polymer films were spin coated onto indium-tin-oxide (ITO)-coated glass substrates, which were cleaned by DMF, acetone, distilled water, and THF sequentially in an ultrasonic bath before use. Residual solvent was removed by heating the films in a vacuum oven at 40 °C.

### 2.9. NLO measurement of poled films

The second-order optical nonlinearity of the polymers was determined by in situ second harmonic generation (SHG) experiment, using a closed temperature-controlled oven with optical windows and three needle electrodes. The films were kept at 45° to

the incident beam and poled inside the oven, and the SHG intensity was monitored simultaneously. Poling conditions were as follows: temperature, different for each polymer (Table 3); voltage, 7.8 kV at the needle point; gap distance, 0.8 cm. The SHG measurements were carried out with a Nd:YAG laser operating at a 10 Hz repetition rate and an 8 ns pulse width at 1064 nm. A Y-cut quartz crystal served as the reference.

## 3. Results and discussion

### 3.1. Synthesis and characterization

The overall pathway of the monomer and polymer synthesis was presented in Schemes 1 and 2. The whole synthetic route utilized some simple reactions, such as azo-coupling reaction, esterification reaction and Sonogashira coupling reaction. The obtained polymers could be readily soluble in common polar organic solvents, including CH<sub>2</sub>Cl<sub>2</sub>, CHCl<sub>3</sub>, THF, DMF and DMSO, making it convenient to test their NLO and other properties.

All the prepared polymers are new compounds, which were characterized by spectroscopic methods, and all gave satisfactory spectral data (see Experimental section and Supporting information for detailed analysis data). Figs. 1 and S1 showed the IR spectra of polymers P1–P4 and chromophores C1–C4, respectively, in which the absorption bands associated with the nitro groups and carbonyl groups were at about 1338, 1517 and 1720 cm<sup>-1</sup>, respectively, showing that the chromophore and isolation groups were stable during the Sonogashira polymerizations. Meanwhile, there was an absorption band derived from the C≡C–H stretching vibrations at about 3277 cm<sup>-1</sup> in the FT-IR spectra of chromophores C3 and C4, while it disappeared in the spectra of its corresponding polymers P1–P4, indicating the successful polymerizations.

Fig. 2 showed the <sup>1</sup>H NMR spectra of C1, C3 and P1, as well as their chemical structures, as an example to illustrate the successful synthesis, while the NMR spectra of other compounds shown in

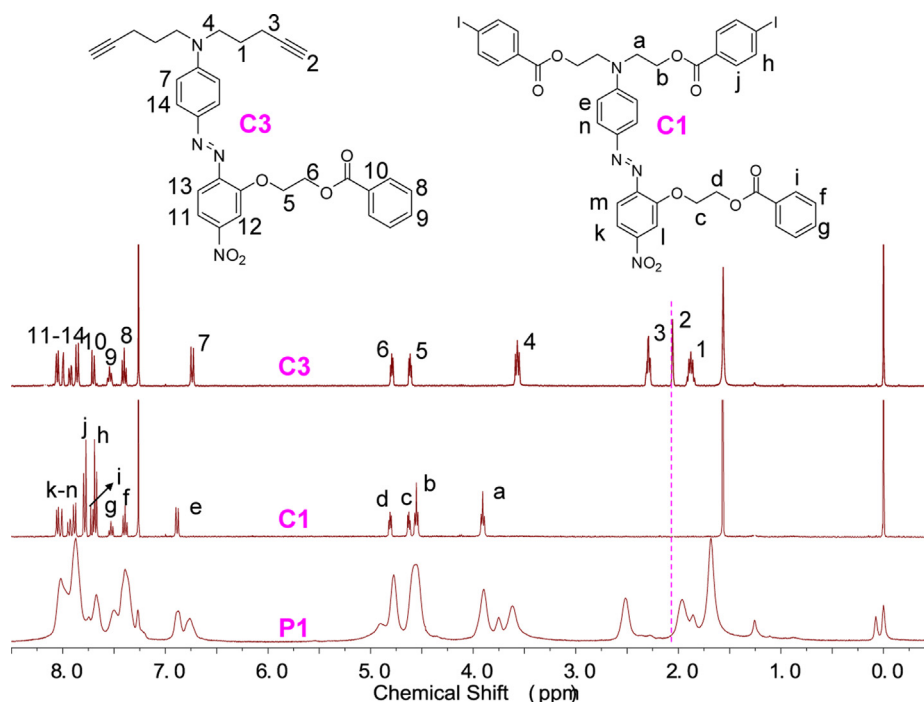


Fig. 2. <sup>1</sup>H NMR spectra of polymer P1 and its corresponding monomers C1 and C3.

**Table 1**  
Characterization data of polymers.

No.	Yield (%)	$M_w^a$	$M_w/M_n^a$	$T_g^b$ (°C)	$T_d^c$ (°C)
<b>P1</b>	72.3	17 200	1.99	105	258
<b>P2</b>	87.7	8200	1.54	135	224
<b>P3</b>	92.4	7200	1.43	111	226
<b>P4</b>	80.7	6600	1.57	100	217

<sup>a</sup> Determined by GPC in THF on the basis of a polystyrene calibration.

<sup>b</sup> Glass transition temperature ( $T_g$ ) of polymers detected by the DSC analyses under argon at a heating rate of 10 °C/min.

<sup>c</sup> The 5% weight loss temperature of polymers detected by the TGA analyses under nitrogen at a heating rate of 10 °C/min.

Figs. S2–S26 in the Supporting information. In the  $^1\text{H}$  NMR spectra of monomers **C1** and **C3**, no unexpected resonance peaks were observed, and the chemical shifts were consistent with the proposed structure (the corresponding peaks were marked in Fig. 1, a–n for **C1** while 1–14 for **C3**). After polymerization, all the peaks of **P1** showed an apparent inclination of signal broadening, and the disappearance of the single peaks associated with the protons of  $\text{C}\equiv\text{CH}$  (marked 2 in **C3**) at 2.06 ppm, confirming the successful polymerization again. The structure of other polymers could be also confirmed similarly. On the other hand,  $^{19}\text{F}$  NMR spectrum was another way to confirm the structures of the monomers and polymers due to the presence of perfluoroaromatic moieties. As shown in Figs. S11 and S16, there were three peaks in the  $^{19}\text{F}$  NMR spectra of chromophores **C2** and **C4**, while no peak in the  $^{19}\text{F}$  NMR spectra of chromophores **4** and **6**, indicating the esterifications were successful. In the same way, the structures of **P2–P4** with pentafluorophenyl as isolation group were confirmed.

The molecular weights of polymers were determined by gel permeation chromatography (GPC) with THF as an eluent and polystyrene standards as calibration standards, with the results summarized in Table 1. Interestingly, under the same polymerization conditions, **P2–P4**, with pentafluorophenyl as isolation group, exhibited much lower molecular weights than **P1**, and the more pentafluorophenyl groups, the lower molecular weights. Considering that under the same polymerization conditions, the only factor to affect the molecular weights was the reaction rate, we could surmise that the introduction of perfluoroaromatic rings would make the reactive activity of Sonogashira reaction a little lower. On the other hand, the low reaction rate usually leads to low yield. However, the yields of **P2–P4** were even higher than that of

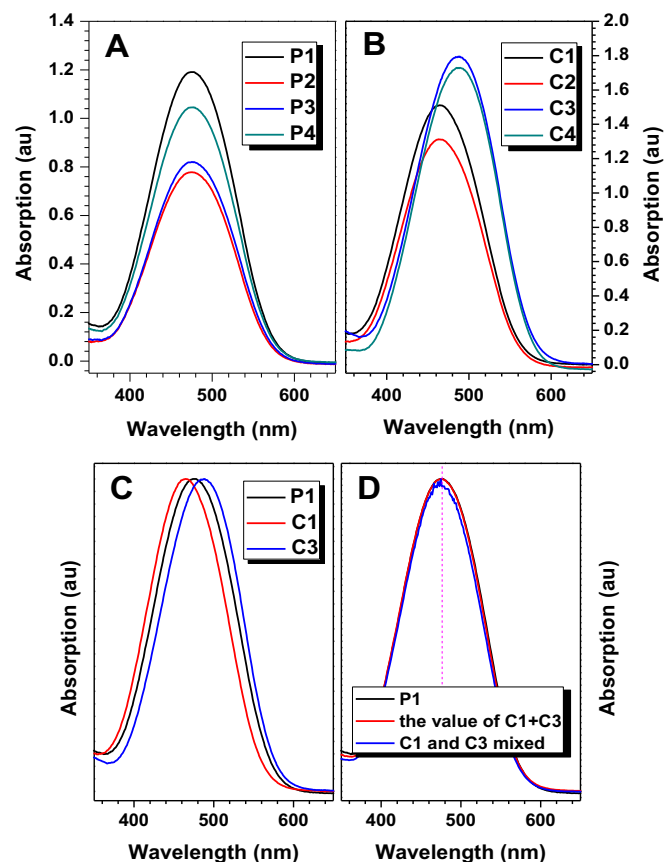


**Fig. 4.** UV–vis spectra in THF solutions: A: polymers **P1–P4** (0.02 mg/mL); B: chromophores **C1–C4** ( $1.0 \times 10^{-5}$  mg/mL); C: normalized absorptions of **P1** and its corresponding monomers; D: normalized absorptions of polymer **P1**, its corresponding monomers **C1** and **C3** ( $1.0 \times 10^{-5}$  mg/mL) mixed with equivalent and the sum value of **C1** and **C3** ( $1.0 \times 10^{-5}$  mg/mL).

**P1**, and it seemed that there was a contradiction to our surmise. But it was not true. In order to improve the performance of the obtained polymers, the precipitation procedure was used to remove the monomers and oligomers. Meanwhile, the chemical structures of these four polymers were not the same exactly, which would result in their different solubility in acetone, the poor solvent used in precipitation. Thus, the final yields of these polymers did not only depend on the reaction rate, but also their solubility, and the effect of solubility should be even more important. Furthermore, the lower polymerization rate of **P2–P4** also indicated that there should be some interactions between the perfluoroaromatic rings and normal aromatic rings in these polymers, which was desirable as expected. Luckily, thanks to their branched structure, the thin films of **P2–P4**, with low molecular weights, could be still easily

**Table 2**  
The maximum absorption of polymers and chromophores ( $\lambda_{\text{max}}$ , nm).<sup>a</sup>

	THF	1,4-Dioxane	Chloroform	Dichloromethane	DMF	DMSO
<b>P1</b>	475	466	475	479	491	498
<b>P2</b>	476	466	477	478	489	497
<b>P3</b>	477	467	476	479	490	496
<b>P4</b>	475	468	477	477	490	497
<b>C1</b>	465	456	461	463	481	487
<b>C2</b>	463	458	459	464	480	486
<b>C3</b>	489	478	493	494	500	507
<b>C4</b>	489	479	493	495	500	507

<sup>a</sup> The maximum absorption wavelength of polymers (chromophore molecules) solutions with the concentrations fixed at 0.02 mg/mL ( $2.5 \times 10^{-5}$  mol/mL).

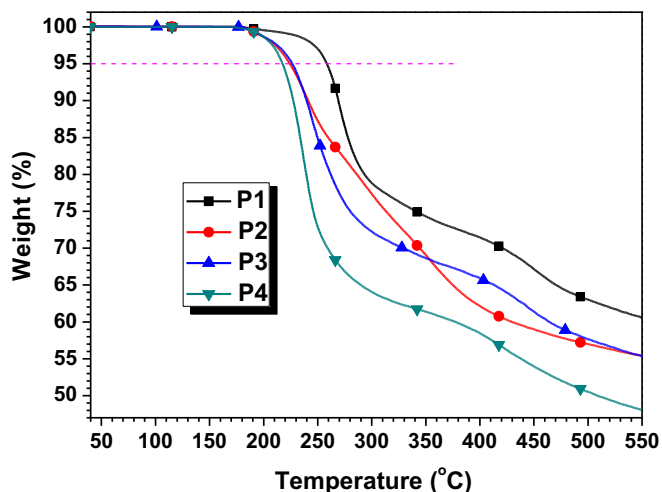


**Fig. 3.** TGA thermograms of **P1–P4**, measured in nitrogen at a heating rate of 10 °C/min.

**Table 3**  
Characterization data of polymers.

No.	$T_g^a$ (°C)	$l^b$ (μm)	$d_{33}^c$ (pm/V)	$d_{33(\infty)}^d$ (pm/V)	$\Phi^e$	$N^f$
<b>P1</b>	110	0.38	100.1	17.1	0.21	0.48
<b>P2</b>	135	0.32	162.3	27.7	0.33	0.45
<b>P3</b>	110	0.31	94.4	16.1	0.15	0.45
<b>P4</b>	95	0.37	150.1	25.6	0.29	0.42

<sup>a</sup> The best poling temperature.

<sup>b</sup> Film thickness.

<sup>c</sup> Second harmonic generation (SHG) coefficient.

<sup>d</sup> The nonresonant  $d_{33}$  values calculated by using the approximate two-level model.

<sup>e</sup> Order parameter  $\Phi = 1 - A_1/A_0$ ,  $A_1$  and  $A_0$  are the absorbance of the polymer film after and before corona poling, respectively.

<sup>f</sup> The loading density of the effective chromophore moieties.

prepared by spin-coating, making it convenient to test their NLO properties.

The TGA thermograms were shown in Fig. 3, and the 5% weight loss temperature ( $T_d$ ) of polymers was listed in Table 1. All the polymers were thermally stable with the  $T_d$  values higher than 217 °C. **P2–P4** exhibited a little worse thermal stability than **P1**, possibly caused by two reasons: first, the pentafluorophenyl group was not so stable as normal phenyl moieties; secondly, the molecular weights of **P1** were much higher than those of **P2–P4**. **P4**, with the lowest molecular weights and containing more pentafluorophenyl groups, thus demonstrated the worst thermal stability. But it should be already enough for NLO materials, because the temperature for its real application was generally lower than 200 °C. The glass transition temperatures ( $T_g$ ) of the polymers were also investigated by using a differential scanning calorimeter (DSC), with the results summarized in Table 1, and all of them showed moderate  $T_g$  in the range of 100–135 °C.

All the polymers were soluble in common polar organic solvents such as  $\text{CHCl}_3$ ,  $\text{CH}_2\text{Cl}_2$ , THF, DMF, and DMSO. The UV–vis absorption spectra of the chromophores and polymers in different solvents were demonstrated in Figs. 4 and S27–S36, and the maximum absorption wavelengths ( $\lambda_{\text{max}}$ ) for the  $\pi$ – $\pi^*$  transitions of the azo moieties were listed in Table 2. Chromophores **C1**, **C2** and **C3**, **C4** consisted of the same nitro acceptor, but different donors, which led to the different  $\lambda_{\text{max}}$  values, as shown in Fig. 4B. It was easily seen that the  $\lambda_{\text{max}}$  of the chromophore moieties in these polymers were nearly the same (Fig. 4A), no matter there were some differences among the four chromophores (Fig. 4C). To investigate the phenomena deeply, the UV–vis absorption spectra of the two corresponding chromophores mixed with equivalent were tested as control experiments, since these polymers consisted of these two types of chromophores equivalently. **P1** and its corresponding chromophores **C1** and **C3** were taken as the example again. As

shown in Fig. 4D, it became obvious that the maximum absorption wavelengths of the chromophore moieties in the polymer of **P1** was nearly the same as the maximum absorption wavelength of the mixture of chromophore **C1** and chromophore **C3** with equivalent. Meanwhile, the sum value of the UV–vis spectra of THF solutions of **C1** and **C3** was also shown as the normalized spectrum in Fig. 4D for reference. The spectrum was nearly the same as the UV–vis absorption spectra of **P1**, indicating the surrounding environment of chromophore moieties did not change much during the polymerization process. Similar phenomena were observed in other polymers (Figs. S37–S39). The almost same  $\lambda_{\text{max}}$ s of these four polymers indicated that the presence of the different isolation spacers nearly did not influence the electronic properties of the chromophore moieties, which would ensure the comparison of their NLO properties on the same level.

### 3.2. NLO properties

To evaluate the NLO activity of these polymers with perfluoroaromatic moieties in different positions, their poled thin films were prepared. The most convenient technique to study the second-order NLO activity was to investigate the second harmonic generation (SHG) processes characterized by  $d_{33}$ , an SHG coefficient. To check the reproducibility, we repeated the measurements at least three times for each sample. Calculation of the SHG coefficients ( $d_{33}$ ) for the poled films was based on the following equation: [11]

$$\frac{d_{33,s}}{d_{11,q}} = \frac{\chi_s^{(2)}}{\chi_q^{(2)}} = \sqrt{\frac{I_s}{I_q} \frac{l_{c,q}}{l_s} F}$$

where  $d_{11,q}$  is  $d_{11}$  of the quartz crystals, which is equal to 0.45 pm/V.  $I_s$  and  $I_q$  are the SHG intensities of the sample and the quartz, respectively,  $l_{c,q}$  is the coherent length of the quartz,  $l_s$  is the thickness of the polymer film, and  $F$  is the correction factor of the apparatus and is equal to 1.2 when  $l_c$  is much greater than  $l_s$ . From the experimental data, the  $d_{33}$  values of **P1–P4** were calculated at a fundamental wavelength of 1064 nm (Table 3). Generally, the  $d_{33}$  value of the same NLO polymer can be different when measured by different methods or different testing systems at different times. To avoid the above-mentioned possible deviations, the NLO properties of all the polymers were tested at the same time.

As shown in Table 3, the  $d_{33}$  values of **P1–P4** were 100.1, 162.3, 94.4 and 150.1 pm/V, respectively. These results were encouraging, and it meant that the perfluoroaromatic isolation groups could lead to higher  $d_{33}$  values than the normal ones, and the  $d_{33}$  value of **P2** was even up to 162.3 pm/V. This was a quite amazing value, since its chromophore moieties were simple azo chromophores [5,9,12].

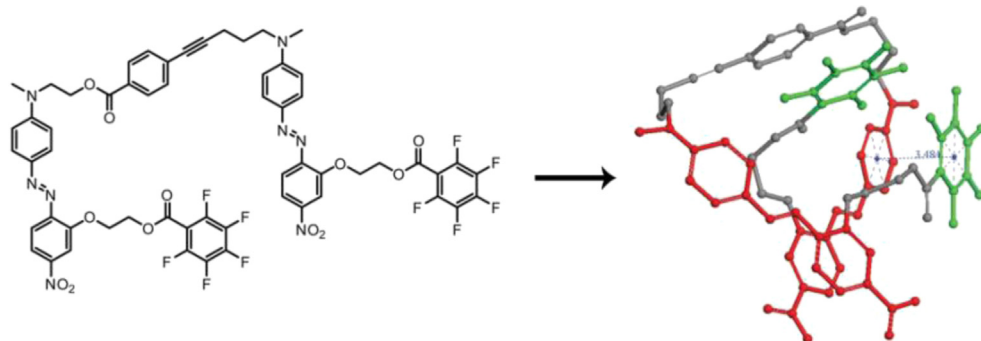


**Fig. 5.** The conformation of dimer that contain perfluoro aromatic isolated spacers.

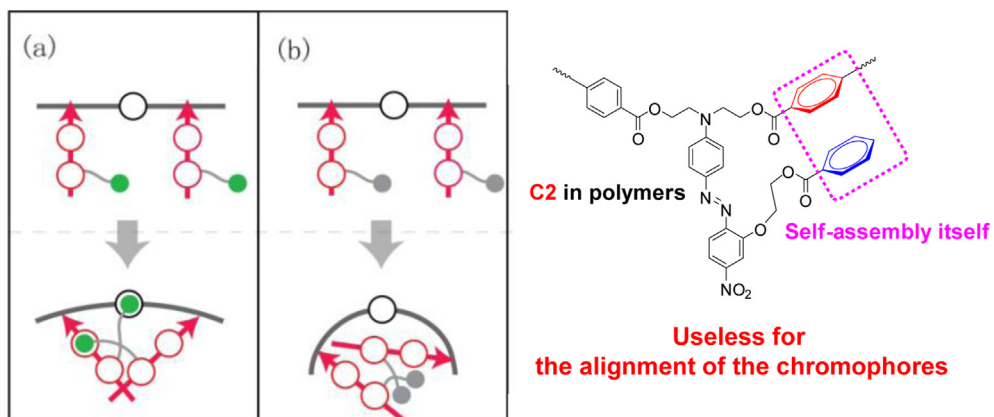
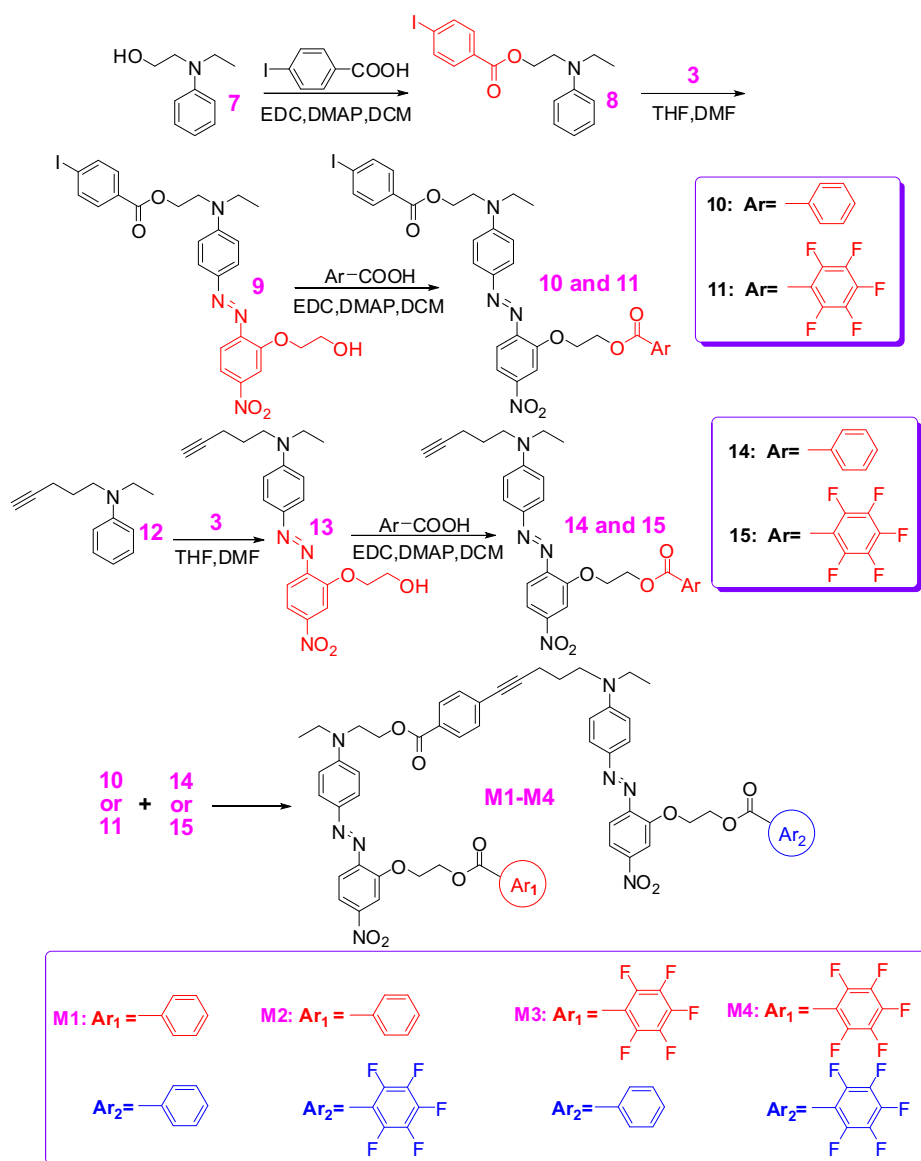


Fig. 6. The abridged general views of the conformation of: (a) polymers with perfluoro aromatic isolation spacers; (b) polymers with normal isolation spacers.



Scheme 3. The synthesis of model molecules M1–M4.

However, not all the perfluoroaromatic isolation spacers could result in higher  $d_{33}$  values: the perfluoroaromatic isolation spacers in chromophore **C2** cause a little lower  $d_{33}$  values, just like **P3** and **P4**.

This abnormal phenomenon should be caused by different interactions between the perfluorophenyl groups and normal phenyl ones at different positions. The different conformations of these polymers caused by Ar–Ar<sup>F</sup> self-assembly effects were therefore considered, which was performed on dimer using Moloc software with MAB forcefield, and the resultant stable conformer was then used repeatedly to construct oligomer (containing 10 monomers). A subsequent molecule dynamics run with opls force field was performed to verify the stability of the oligomers, with the results shown in Figs. 5 and 6. Due to the different self-assembled effects, the conformations of polymers were different. The perfluoroaromatic rings in chromophore **C2**, which still had another normal phenyl groups as isolation groups, could self-assemble with the normal isolation group by itself. This should be therefore useless for the alignment of chromophores, however, making the loading density of the effective chromophore moieties lower, since the relative atomic mass of F atom was much larger than H atom (Table 3). And it was well-known that in theory, under identical experimental conditions, the  $d_{33}$  value was proportional to the density of the chromophore moieties. Thus, the  $d_{33}$  value of **P4** was a little lower than that of **P2**, and the  $d_{33}$  value of **P3** was a little lower than that of **P1**. On the contrary, in chromophore **C4**, the self-assembly effect could occur between the perfluorophenyl group in **C4** and another chromophore moiety, which could make the alignment of chromophore moieties much easier (Fig. 5A. Meanwhile, Fig. 5B showed the conformation of polymers with normal isolation spacers for comparison), thus, further increasing the NLO coefficient in a large degree.

To aid the investigation of these different Ar–Ar<sup>F</sup> self-assembly effect in depth, four model molecules **M1–M4** (Scheme 3), with the similar structure to **P1–P4** (see Supporting information for their synthetic procedure), were also synthesized. However, it was a pity that no useful information was obtained (including NMR, FT-IR spectra and the melting point, etc. see Experimental section and Supporting information for detail). Thus, further researches were still needed, to find more evidence to check the different Ar–Ar<sup>F</sup> self-assembly effect, and to apply this effect to other NLO chromophores with higher  $\mu\beta$  values, with the aim for larger NLO coefficients. These researches were in progress in our laboratory.

As there might be some resonant enhancement due to the absorption of the chromophore moieties at 532 nm, the NLO properties of **P1–P4** should be much smaller (Table 3, ( $d_{33}(\infty)$ )), which were calculated by using the approximate two-level model. Since all the polymers exhibited nearly the same UV–vis absorption behavior, their  $d_{33}(\infty)$  values demonstrated the same phenomena as their  $d_{33}$  values.

To further study the alignment behavior of the chromophore moieties in **P1–P4**, their order parameter ( $\Phi$ ) (Table 3) was also measured and calculated from the change of the UV–vis spectra of their films before and after poling under electric field (Figs. S40–S43), according to the equation described in Table 3 (footnote e). The tested  $\Phi$  values were in accordance with their  $d_{33}$  and  $d_{33}(\infty)$  values: **P2** and **P4** exhibited higher  $\Phi$  values (0.33 and 0.29 respectively) than those of **P1** and **P3** (0.21 and 0.15 respectively), indicating that much effective oriented alignment of the dipole moments was achieved in **P2** and **P4**, further confirming the above discussions.

The dynamic thermal stabilities of the NLO activities of the polymers were investigated by depoling experiments, in which the real time decays of their SHG signals were monitored as the poled films were heated from 35 to 140 °C in air at a rate of 4 °C/min. Fig. 7 showed the decay of SHG coefficient of all the polymers as a function of temperature. Since the  $T_g$  value of **P2** was the highest

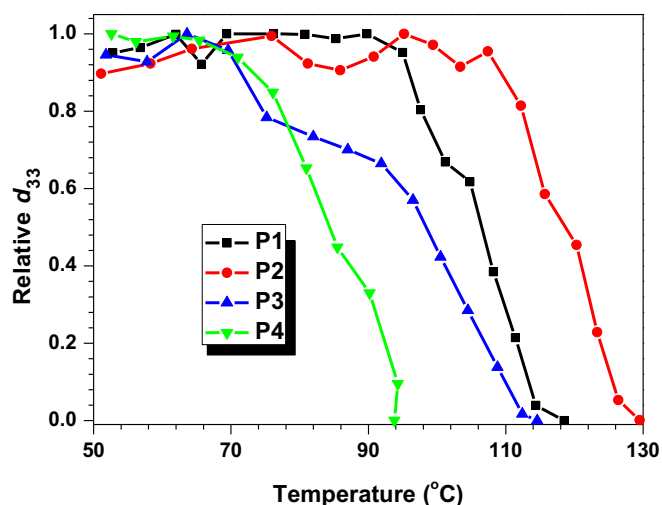


Fig. 7. Decay curves of the SHG coefficients of **P1–P4** as a function of the temperature.

one, it still has the highest onset temperature for decay in the  $d_{33}$  value as 111 °C, thanks to the Ar/Ar<sup>F</sup> interactions. However, it was not so clear how these Ar/Ar<sup>F</sup> interactions affect the  $T_g$  values of NLO polymers, for example, the  $T_g$  values of **P3** and **P4** did not demonstrate advantages in comparison with that of **P1**, and the onset temperatures for decay were also lower than that of **P1**. Thus, further researches were still needed, to make the effect of these interactions to  $T_g$  values of polymers much clear. That was to say, the self-assembly effect in the NLO polymers in **P2** could lead to the better stability. Anyhow, in **P2**, which demonstrated the highest NLO coefficient in these polymers, the self-assembly effect also brought out the best stability, making it good candidate for the practical applications.

#### 4. Conclusion

In this work, four new polyaryleneethynyls **P1–P4** were successfully prepared via the simple palladium-catalyzed Sonogashira coupling reaction, in which the Ar–Ar<sup>F</sup> interaction was used to improve the poling efficiency of these NLO polymers. The preliminary results demonstrated that the concentration and position of perfluoroaromatic isolation groups in the chromophore could affect the NLO effect of the corresponding polymers largely. **P2** demonstrated the largest NLO effect of 162.3 pm/V. Coupled with its better stability, **P2** would be a good candidate for the practical applications. Thus, our study might provide some new useful information on the design of new NLO polymers with better NLO properties by using the higher  $\mu\beta$  value chromophores.

#### Acknowledgments

We are grateful to the National Science Foundation of China (no. 21034006) for financial support.

#### Appendix A. Supplementary material

Supplementary material related to this article can be found at <http://dx.doi.org/10.1016/j.polymer.2013.07.073>.

#### References

- [1] (a) Shi Y, Zhang C, Zhang H, Bechtel JH, Dalton LR, Robinson BH, et al. Science 2000;288:119;

- (b) Lee M, Katz HE, Erben C, Gill DM, Gopalan P, Heber JD, et al. *Science* 2002;298:1401;
- (c) Marder SR, Kippelen B, Jen AKY, Peyghambarian N. *Nature* 1997;388:845;
- (d) Dalton LR, Steier WH, Robinson BH, Zhang C, Ren A, Garner S, et al. *J Mater Chem* 1999;9:1905;
- (e) Kajzar F, Lee KS, Jen AKY. *Adv Polym Sci* 2003;161:1;
- (f) Luo JD, Zhou XH, Jen AKY. *J Mater Chem* 2009;19:7410;
- (g) Dalton LR, Sullivan PA, Bale DH. *Chem Rev* 2010;110:25.
- [2] (a) Robinson BH, Dalton LR. *J Phys Chem A* 2000;104:4785;
- (b) Pereverzev YV, Prezhdo OV, Dalton LR. *Chem Phys Chem* 2004;5:1821;
- (c) Ma H, Liu S, Luo J, Suresh S, Liu L, Kang SH, et al. *Adv Funct Mater* 2002;12:565;
- (d) Fusco S, Centore R, Riccio P, Quatela A, Stracci G, Archetti G, et al. *Polymer* 2008;49:186;
- (e) Yesodha SK, Pillai CKS, Tsutsumi N. *Prog Polym Sci* 2004;29:45.
- [3] (a) Liao Y, Anderson AA, Sullivan PA, Akelaitis AJP, Robinson BH, Dalton LR. *Chem Mater* 2006;18:1062;
- (b) Sullivan PA, Akelaitis AJP, Lee SK, McGrew G, Choi DH, Dalton LR. *Chem Mater* 2006;18:344;
- (c) Ma H, Chen BQ, Sassa T, Dalton LR, Jen AKY. *J Am Chem Soc* 2001;123:986;
- (d) Luo J, Liu S, Haller M, Liu L, Ma H, Alex JKY. *Adv Mater* 2002;14:1763.
- [4] (a) Fréchet JMJ, Henmi M, Gitsov I, Aoshima S, Leduc MR, Grubbs RB. *Science* 1995;269:1080;
- (b) Fréchet JMJ, Hawker CJ, Gitsov I, Leon JWJ. *Macromol Sci Pure Appl Chem* 1996;33:1399.
- [5] (a) Li Z, Li Q, Qin J. *Polym Chem* 2011;2:2723;
- (b) Li Z, Li Z, Di C, Zhu Z, Li Q, Zeng Q, et al. *Macromolecules* 2006;39:6951;
- (c) Zeng Q, Li Z, Li Z, Ye C, Qin J, Tang B. *Macromolecules* 2007;40:5634;
- (d) Li Z, Dong S, Yu G, Li Z, Liu Y, Ye C, et al. *Polymer* 2007;48:5520;
- (e) Li Z, Li P, Dong S, Zhu Z, Li Q, Zeng Q, et al. *Polymer* 2007;48:3650;
- (f) Li Z, Wu W, Qin J, Ye C, Qin J, Li Z. *Polymer* 2012;53:153;
- (g) Li Z, Wu W, Li Q, Yu G, Xiao L, Liu Y, et al. *Angew Chem Int Ed* 2010;49:2763;
- (h) Wu W, Huang L, Song C, Yu G, Ye C, Liu Y, et al. *Chem Sci* 2012;3:1256;
- (i) Wu W, Wang C, Zhong C, Ye C, Qiu G, Qin J, et al. *Polym Chem* 2013;4:378;
- (j) Wu W, Ye C, Qin J, Li Z. *Polym Chem* 2013;4:2361;
- (k) Li Z, Yu G, Li Z, Liu Y, Ye C, Qin J. *Polymer* 2008;49:901;
- (l) Li Q, Li Z, Ye C, Qin J. *J Phys Chem B* 2008;112:4928;
- (m) Li Q, Yu G, Huang J, Liu H, Li Z, Ye C, et al. *Macromol Rapid Commun* 2008;29:798;
- (n) Li Q, Li Z, Zeng F, Gong W, Li Z, Zhu Z, et al. *J Phys Chem B* 2007;111:508;
- (o) Li Z, Zeng Q, Yu G, Li Z, Ye C, Liu Y, et al. *Macromol Rapid Commun* 2008;29:136.
- [6] (a) Jang SH, Jen AKY. *Chem Asian J* 2009;4:20;
- (b) Coates GW, Dunn AR, Henling LM, Dougherty DA, Gubbs RH. *Angew Chem Int Ed* 1997;36:248;
- (c) Patrick CR, Prosser GS. *Nature* 1960;187:1021.
- [7] (a) Kim TD, Kang J, Luo J, Jang S, Ka J, Tucker N, et al. *J Am Chem Soc* 2007;129:488;
- (b) Gray T, Kim TD, Knorr Jr DB, Luo J, Jen AKY, Overney RM. *Nano Lett* 2008;8:754.
- [8] Zhou X, Luo J, Huang S, Kim TD, Shi Z, Cheng Y, et al. *Adv Mater* 2009;21:1976.
- [9] (a) Wu W, Huang Q, Qiu G, Ye C, Qin J, Li Z. *J Mater Chem* 2012;22:10486;
- (b) Wu W, Zhu Z, Qiu G, Ye C, Qin J, Li Z. *J Polym Sci Part A: Polym Chem* 2012;50:5124;
- (c) Wu W, Fu Y, Wang C, Ye C, Qin J, Li Z. *Chem Asian J* 2011;6:2787;
- (d) Wu W, Yu G, Liu Y, Ye C, Qin J, Li Z. *Chem Eur J* 2013;19:630;
- (e) Wu W, Wang C, Tang R, Fu Y, Ye C, Qin J, et al. *J Mater Chem C* 2013;1:717.
- [10] Zhu Z, Li Q, Zeng Q, Li Z, Li Z, Qin J, et al. *Dyes Pigments* 2008;78:199.
- [11] (a) Li Z, Huang C, Hua J, Qin J, Yang Z, Ye C. *Macromolecules* 2004;37:371;
- (b) Li Z, Qin J, Li S, Ye C, Luo J, Cao Y. *Macromolecules* 2002;35:9232;
- (c) Li Z, Gong W, Qin J, Yang Z, Ye C. *Polymer* 2005;46:4971;
- (d) Li Z, Hua J, Li Q, Huang C, Qin A, Ye C, et al. *Polymer* 2005;46:11940;
- (e) Li Z, Li J, Qin J, Qin A, Ye C. *Polymer* 2005;46:363;
- (f) Li Z, Wu W, Ye C, Qin J, Li Z. *Polymer* 2012;53:153.
- [12] (a) Scarpaci A, Blart E, Montebault V, Fontaine L, Rodriguez V, Odobel F. *ACS Appl Mater Inter* 2009;1:1799;
- (b) Scarpaci A, Blart E, Montebault V, Fontaine L, Rodriguez V, Odobel F. *Chem Commun* 2009;14:1825;
- (c) Wu W, Ye C, Yu G, Liu Y, Qin J, Li Z. *Chem Eur J* 2012;18:4426;
- (d) Wu W, Li C, Ye C, Yu G, Liu Y, Qin J, et al. *Chem Eur J* 2012;18:11019;
- (e) Xie J, Hu L, Shi W, Deng X, Cao Z, Shen Q. *J Polym Sci Part B: Polym Phys* 2008;46:1140;
- (f) Chang H, Chao T, Yang C, Dai S, Jeng R. *Eur Polym J* 2007;43:3988.